Spirals on the sea: A manifestation of upper-ocean stirring

Walter Munk and Laurence Armi

Scripps Institution of Oceanography, La Jolla, California

Abstract. Spiral eddies were first seen in the sun glitter on the Apollo Mission 30 years ago; they have since been recorded on SAR missions and in the infrared. The spirals are globally distributed, 10–25 km in size and overwhelmingly cyclonic. They have not been explained. Under light winds favorable to visualization, linear surface features with high surfactant density and low surface roughness are of common occurrence. We have proposed that frontal formations concentrate the ambient shear and prevailing surfactants. Horizontal shear instabilities ensue when the shear becomes comparable to the Coriolis frequency. The resulting vortices wind the linear features into spirals. The hypothesis needs to be tested by prolonged measurements and surface truth. Spiral eddies are a manifestation of a sub-mesoscale oceanography associated with upper ocean stirring; dimensional considerations suggest a horizontal diffusivity of order $10^3 \mathrm{m}^2\mathrm{s}^{-1}$.

Introduction

The first photographs of spiral eddies appears to have been taken on Apollo-Saturn in October 1968. In the late 70s SEASAT with its synthetic aperture radar (SAR) confirmed the early discoveries from crewed space flights (*Stevenson* 1998, 1999). But most of the existing material was collected by Paul Scully-Power (the first and so far only oceanographer-astronaut) on 5–13 October 1984: "Far and away the most impressive discovery... is that of the submesoscale ocean (less than 100 km) is far more complex dynamically than ever imagined... Patterns of this complexity could be seen to be interconnected for hundreds and hundreds of kilometers" (*Scully-Power* 1986).

The spiral pattern whose global distribution was reported by Scully-Power is at an awkward scale, virtually impossible to recognize from shipboard, and too large to be encompassed even from high-flying aircraft. Discovery had to await space missions.

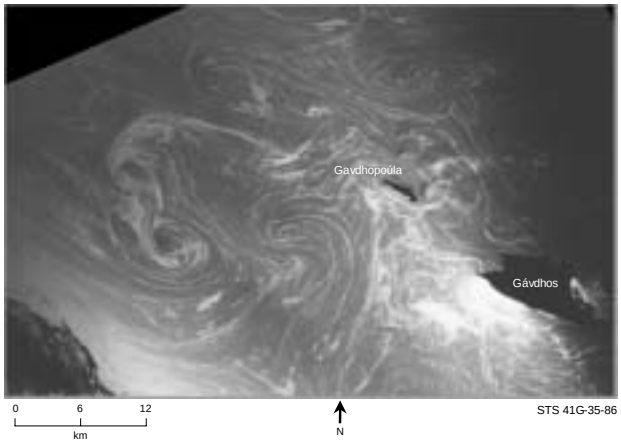

Figure 1. A pair of interconnected spirals in the Mediterranean Sea south of Crete. This vortex pair has a clearly visible stagnation point between the two spirals, the cores of which are aligned with the preconditioning wind field. 7 October 1984.

Spiral Images in the Sun Glitter and in SAR

Figures 1 and 2 show a visual and SAR image, respectively, of spiral streak patterns. Spirals are globally distributed (Figure 3). Typical spiral dimensions are from 10 to 20 km, with streaks 50 to 100 m wide. Spirals are overwhelmingly cyclonic, wound anti-clockwise (viewed from above) in the northern hemisphere, clockwise in the southern hemisphere. Ship wakes crossing the streaks (not shown) have a cyclonic offset with shears up to $10^{-3}\mathrm{s}^{-1}$. We need to refer to *Munk et al.* (2000) (henceforth *MAFZ*) for a more representative selection (13 images out of 400 collected).

The observational material poses three questions:

(A) How are the spirals wound?

(B) How is symmetry broken in favour of cyclonic rotation?

(C) What makes spirals visible?

On SAR images the streaks are always dark, indicat-

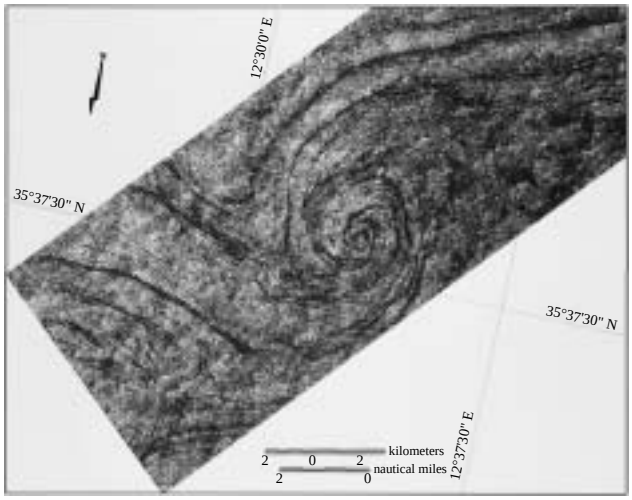

Figure 2. Spirals in the Mediterranean Sea visualized with Shuttle XSAR. The streaks are differentially smooth. 9 October 1994.

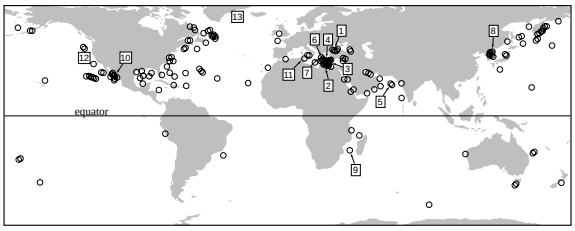

Figure 3. Distribution of spiral eddies from *Scully-Power* (1986) visual observations and our collection of 400 images. The 13 numbered locations refer to *MAFZ*.

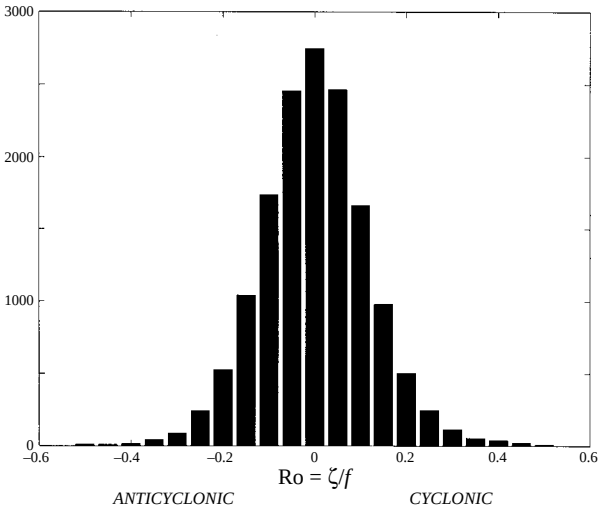

Figure 4. Rossby number in the upper 250 m sampled at 3 km spacing along 140° W from 25° N to 35° N in the North Pacific (*Rudnick and Ferrari* 1999).

ing a reduced scattering cross-section, e.g. differentially smooth water. Natural biogenic surface films are organized by near-surface convergence into linear streaks with over 40% surfactant coverage at low winds. The concentration is associated with nearly inextensible surface films which dissipate capillaries and short gravity waves. The film thickness required to dampen the short waves is only 0.01 to 0.1 μm. On the optical images the smooth streaks are bright in the inner sun glitter (which requires low rms slopes for reflection of the sun into the camera) and dark in the outer glitter. The situation is complex and not well understood, and we refer to *MAFZ* (1225-30, 1236-7) for further discussion.

But evidently the third question can be restated as follows: What is the circulation pattern that collects the surfactant material into streaks (which are subsequently wound into a spiral pattern)? Multiple stripes at kilometer spacing presumably are associated with helical circulation rolls in the atmospheric boundary layer. In addition, frontal instabilities can concentrate and distort the surfactant, as we shall see.

Ambient Ocean Vorticity

Measurement of surface velocity shear du/dy along 1000 km of roughly northward track in the North Pacific (*Rudnick and Ferrari* 1999) indicate values of order $10^{-5}\mathrm{s}^{-1}$. The situation is conveniently portrayed by a distribution of Rossby Numbers

$$\mathrm{Ro} = \zeta/f \tag{1}$$

where $\zeta = \partial v/\partial x - \partial u/\partial y$ is the vertical component of vorticity (cyclonic is positive) and f is the Coriolis frequency (Figure 4). The distribution is symmetric, with very few values exceeding $\frac{1}{4}$. There are a few outliers showing a slight preference of cyclonic vorticity for large |Ro|, and this has since been confirmed (*Rudnick*, this volume).

The above paper also shows that the shear is distributed over a broad band of scales, from kilometers to hundreds of kilometers.

Horizontal Shear Instability

Starting from parallel shear flow with an inflection point, Figure 5 shows a numerical simulation of the development of the most unstable mode (*Corcos and Sherman* 1976, 1984). Time is in units of the initial reciprocal shear at the stagnation point The numerical experiment was intended to model a vertical shear flow, but may as well be interpreted in terms of a horizontal shear flow. There is no implication of the sense of rotation; in fact we have reversed the published drawing from anticyclonic to cyclonic rotation.

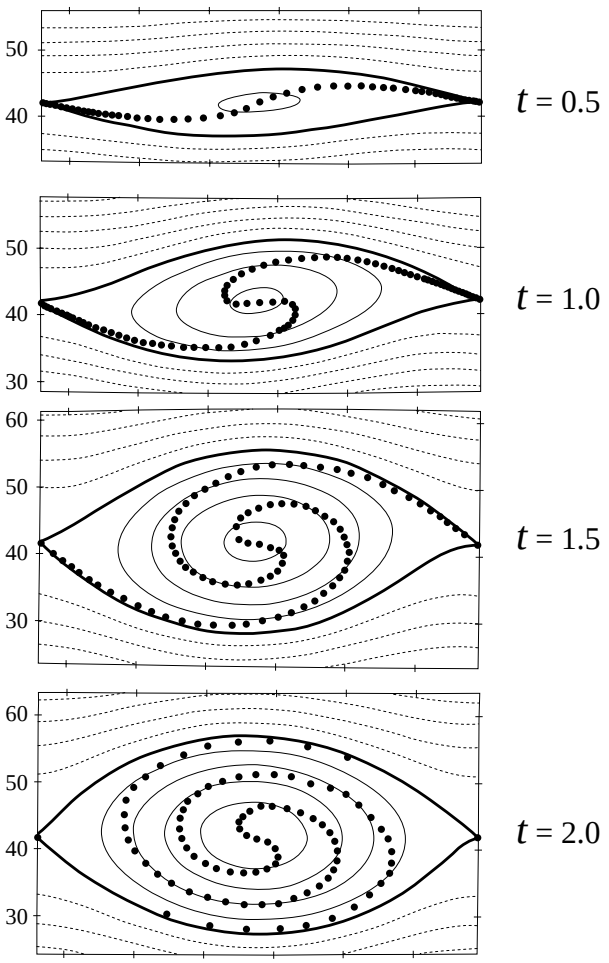

Figure 5. Computer simulations of a developing shear instability (*Corcos and Sherman* 1984). The four panels show the streamlines at times 0.5, 1.0, 1.5, 2.0 (in units of the initial reciprocal shear). Heavy line is the "cat's-eye" streamline through the stagnation points. The dots represent particle positions initially placed on the interface; they are initially crowded near the two stagnation points to allow for a subsequent large strain. The model allows for diffusion and viscosity. We have reversed the original figure from anticyclonic to cyclonic rotation.

Streamlines show the development of Kelvin's celebrated "cat's-eye" solution. Particles inserted along the interface exhibit the growth of a spiral.

It is instructive to compare this numerical experiment with *Stuart's* (1967) steady-state solution for a non-rotating incompressible equal-density fluid (Figure 6). The streamlines are given by

$$\Psi(x,y) = -k^{-1}U\log(\cosh ky - \alpha\cos kx). \qquad (2)$$

For $\alpha = 0$ we have $u = -\partial\Psi/\partial y = -U\tanh ky$. It is readily shown that vorticity is conserved:

$$D\zeta/Dt = 0, \quad \zeta = -\nabla^2\Psi \qquad (3)$$

where D/Dt is the substantial derivative (following a particle). The circulation $\Gamma = \int \zeta\, dx\, dy = 4\pi\, U\, k^{-1}$ is the same for all four panels. The streamlines through the two stagnation points separate the "core circulation" from an exterior circulation which is not all that different from the case $\alpha = 0$. The fractional core circulation

$$\Gamma_C/\Gamma = 4\pi^{-1}\tan^{-1}\sqrt{a} \qquad (4)$$

increases with increasing α. The four panels give independent steady-state solutions for different values of the independent parameter α, but we are tempted, by comparison of the two figures, to interpret the Stuart solution as a developing instability for a slowly increasing $\alpha(t)$. In *MAFZ* we demonstrate that an initial particle injection produces mature spirals, as in the Corcos and Sherman numerical experiment, some of them resembling the vortex pair in the Cretan Sea (Figure 1). The proposed response to question A is that the spirals are a manifestation of a horizontal shear instability.

There is as yet no breaking of symmetry. In fact, replacing $D\zeta/Dt = 0$ by

$$D(\zeta + f)/Dt = 0 \qquad (5)$$

does not change the developing streamline pattern, so that planetary vorticity is conserved in the f-plane. But the developing pressure patterns are fundamentally modified (*MAZD* figure 22). Starting with the Stuart solution of a low pressure in the core (regardless of the sense of rotation) and gradually turning on the coriolis parameter f, the core pressure remains a LOW for the cyclonic case but switches to a HIGH for the anticyclonic case. Clearly there is here the dynamics for breaking symmetry.

Breaking Symmetry: the Hoskins-Bretherton Jet

Hoskins and Bretherton (1972) have solved a problem of frontogenesis with conservation of density and potential vorticity,

$$D(\rho,\ q)/Dt = 0, \quad \rho\, q = (f+\zeta)\bullet\nabla\rho \qquad (6)$$

where D/Dt is the substantial derivative. The starting point is a vertically mixed layer with a horizontal density transition from warm and light in the south (say) to cold and heavy in the north (Figure 7, left). The initial density gradient develops into an eastward "thermal wind", as shown. A deformation field γ =

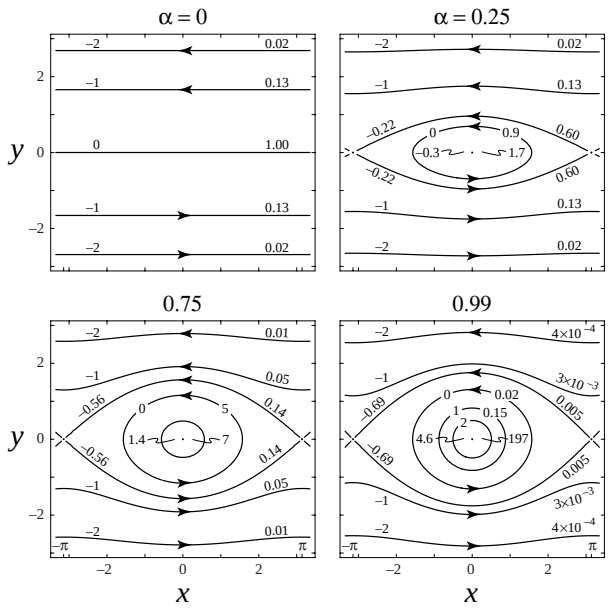

Figure 6. *Stuart's* (1967) solution portraying a steady flow conserving vorticity. Streamlines designate both dimensional streamlines $\Psi = -\log q$, $q = \cosh y - \alpha \cos x$), and lines of constant vorticity $\zeta = (1-\alpha^2)q^{-2}$, with values indicated in each panel to the left and right, respectively. For $\alpha = 0$ the velocity profile is $u = -\tanh y$. Stagnation points at $x = \pm\pi$, $y = 0$ are connected by the stagnation stream lines separating the closed "core" circulation from the outer flow. With increasing α a larger fraction of the circulation is concentrated within the core.

$\partial u/\partial x - \partial v/\partial y$ is superposed, causing the initially vertical isopycnals to tilt northward. Up to this point there has been no breaking of symmetry, all directions can be reversed.

In the subsequent development we use "north" and "east" only for convenient reference to the figure. The northward tilting of isopycnals is not uniform; the northern isopycnals converge at the surface, and the southern isopycnals diverge. Accordingly the associated eastward thermal jet has a strong cyclonic shear at its northern (left) flank and a weak anticyclonic shear at its southern (right) flank. At time 2.5 (measured in γ^{-1} units) the associated Rossby numbers are $\mathrm{Ro}^+ = +1$ and $\mathrm{Ro}^- = -0.3$, respectively.

At this stage the underlying rate of strain no longer determines the rate of development. Rather, the isopycnal "collapse" takes the form of a "Rossby Adjustment Problem" with $f^{-1} \approx 10^{-4}\mathrm{s}^{-1}$ taking the place of $\gamma^{-1} \approx 10^{-5}\mathrm{s}^{-1}$ as the relevant time scale (*Ou* 1984). In the short time interval between 2.5 to 2.75 γ^{-1} the cyclonic shear grows from $\mathrm{Ro}^+ = 1$ to $\mathrm{Ro}^+ = 3$, and at 2.89 γ^{-1} the density gradient at the left flank develops $\mathrm{Ro}^+ = \infty$, while anticyclonic shear remains at $\mathrm{Ro}^- = -0.3$.

The crucial point is that starting at a time when Ro^+ is of order +1 the cyclonic shear zone becomes a breeding ground for spiral eddies long before appreciable anticyclonic vorticity has been generated. In Figure 4 the third panel has been emphasized because at this time the vertical shear at the surface at the front reaches a value of $du/dz = 2N$ (N is the buoyancy frequency) corresponding to a Richardson number $(N/(du/dz))^2 = \frac{1}{4}$ and suggesting the onset of vertical shear instability.

An independent consideration has to do with the visibility of the spiral arms, presumably the result of the alignment and concentration of surfactants. Consider an elementary surface area $\delta x \delta y$ at time zero. With the developing front the area is elongated along the x-axis on both flanks of the developing jet. But in accordance with the Hoskins and Bretherton theory, at the time 2.75 γ^{-1} the area has *expanded* (by a factor $\frac{7}{4}$) on the anticyclonic side, while it has *contracted* (to $\frac{1}{4}$ the original area) on the cyclonic side. Thus the frontal theory has the elements to account for both the visibility and sense of rotation of the spiral eddies. But when examined in detail the story is not as clear-cut as presented here, and we must refer to *MAFZ* for a more complete discussion.

Breaking Symmetry: the Margules Front

In the traditional Margules treatment of a sharp front, anticyclonic fronts are ruled out by the condition of static stability. For a "softened Margules front" (*MAFZ*) there is a gravitational stability limit to the anticyclonic shear, but no such limit to the cyclonic case.

Breaking Symmetry: Anticyclonic Instabilities

To further confuse the issue, there is another independent set of processes to explain the dominance of cyclonic vortices. It follows from the Rayleigh criterion of stability (extended to include Coriolos acceleration) that cyclonic circular vortices are stable and anticyclonic vortices are unstable (*MAFZ* 6.21), and this leads to an "inertial instability" criterion $\mathrm{Ro} < -1$ which goes back to *Pedley* (1969). Oceanographers are familiar with the vertical shear (Richardson) instability for $\mathrm{d}u/dz > 2N$ but surprisingly unfamiliar with the horizontal shear (Pedley) instability for $du/dy > f$.

There is ample numerical evidence for instabilities

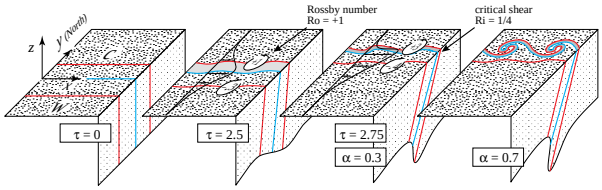

Figure 7. Cartoon for the generation of ocean spirals (see text).

that impede the development of anticyclonic vortices but have no such effect on cyclonic vortices. (*Lesieur et al.,* 1991, *Potylitsin and Peltier* 1998). The distinction is equally clear in laboratory experiments (*Bidokhti and Tritton* 1992). *Kloosterziel* (1990) observed that "it is virtually impossible to create anticyclonic vortices ...by simply stirring the fluid locally. But cyclonic vortices are easily created in this way! In the anticyclonic case stirring .... leads to turbulent motion and the generation of waves whereas by cyclonic stirring a well-defined smooth vortex forms."

With regard to question B, it is unresolved whether the dominance of cyclonic vortices is associated with a dominance in cyclonic horizontal shear early in the formation process, or with the relative instability of anticyclonic vortices in the mature stage.

Stirring and Mixing

The proposed formation of spiral eddies is cartooned in Figure 7. The geostrophically balanced ambient ocean vorticity of order $\pm 10^{-1} f$ is enhanced by local frontogenic processes, with concentration of surfactant along a converging line. When the frontal shear becomes comparable to f, instabilities lead to cross-frontal flow accompanied by a cat's-eye circulation pattern. The cat's-eye circulation twists the convergence line and neighboring linear features into a cyclonic spiral which stretches and further thins the lines of surfactant concentration. It is a text-book example of horizontal stirring.

We have not made any serious attempt at estimating the relevant diffusivity. The best we can do is a dimensional argument for $\kappa = c l' u'$ with $c = \frac{1}{4}$ (typical for turbulent shear flows, *Tennekes and Lumley* 1972). Taking the minor axis of a Stuart core as the characteristic length l', the maximum velocity along the stagnation streamline for u' and $\alpha = 1$ for a mature 20 km spiral yields $\kappa = 10^3 \mathrm{m}^2\ \mathrm{s}^{-1}$ (*MAFZ*).

Testing the Hypothesis

Our hypothesis is based on observational material which consists almost entirely of unrelated glimpses in x, y-space on the sea surface. For a satellite in a low earth orbit (LEO) a given point remains within view for only about 6 s. What is required here are prolonged stares or frequent repeat visits coordinated with shipboard observations (Figure 8). We cannot think of any x, y, z, t ocean processes that had been properly identified from measurements in half the coordinate space. We must assume that there are serious flaws in the foregoing presentation.

Figure 8. The proposed experiment. SAR imagery from an overhead drone is examined by the authors on shipboard in real time. The image shows the position of the vessel which is about to enter a spiral streak.

Following his 41-G space mission in October 1984. *Scully-Power* (1986) wrote: "The almost ubiquitous occurrence (of spiral eddies), whenever submesoscale dynamics was revealed in the sun glitter, indicates that they are perhaps the most fundamental entity in ocean dynamics at this scale. The difficulty is in explaining their structure." The only serious attempt at analysis has been in a Norwegian Doctoral dissertation which explores baroclinic instabilities in a narrow cyclonic shear

zone (*Eldevik and Dysthe* 1999). Why has the problem received so little attention in the thirty years since discovery? We assert that the fashion during these years has been statistical rather than phenomenological descriptions of ocean features, and here we are concerned with a truly phenomenological problem.

References

Bidokhti, A.A., and D.J. Tritton, The structure of a turbulent free shear layer in a rotating fluid. *J. Fluid Mech., 241*, 469-502, 1992.

Corcos, G.M., and F.S. Sherman, Vorticity concentration and the dynamics of unstable free shear layers. *J. Fluid Mech., 73*, 241-264, 1976.

Corcos, G.M., and F.S. Sherman, The mixing layer: deterministic models of a turbulent flow. Part I. Introduction an d the two-dimensional flow. *J. Fluid Mech., 139*, 29-65, 1984.

Eldevik, T., and K.B. Dysthe, Short frontal waves: can frontal instabilities generate small scale spiral eddies, *Selected Papers of the ISOFRP* (ed. A. Zatsepin and A. Ostrovskii), ONESCO, 1999.

Hoskins, B.J., and F.P. Bretherton, Atmosphere frontogenesis models: mathematical formulation and solution. *J. Atmos. Sci., 29*, 11-37, 1972.

Kloosterziel, R.C., Barotropic vortices in a rotating fluid. Phd thesis, University of Utrecht, the Netherlands, 1990.

Lesieur, M., S. Yanase, and O. Métais, Stabilizing and destabilizing effects of a solid-body rotation upon quasi-two-dimensional shear layers. *Phys. Fluids A, 3*, 403-407, 1991.

Munk W, L. Armi, K. Fischer, and F. Zachariasen, Spirals on the Sea. *Proc. R. Soc. London A, 456*, 1217-1280, 2000.

Ou, Hsien Wang, Geostrophic Adjustment: A Mechanism for Frontogenesis. *J. Phys. Oceanogr., 14*, 994-1000, 1984.

Pedley, T.J., On the stability of viscous flow in a rapidly rotating pipe. *J. Fluid Mech., 36*, 177-222, 1969.

Potylitsin, P.G., and W.R. Peltier, Stratification effects on the stability of columnar vortices of the f-plane. *J. Fluid Mech., 355*, 45-79, 1998.

Rudnick, D.L., and R. Ferrari, Compensation of horizontal temperature and salinity gradients in the ocean mixed layer. *Science, 283*, 526-529, 1999.

Scully-Power, P., Navy Oceanographer Shuttle observations, STS 41-G Mission Report. Naval Underwater Systems Center, NUSC Technical Document 7611, 1986.

Stevenson, R.E., Spiral eddies: the discovery that changed the face of the oceans. *21st Century Sci. Technol., 11*, 58-71, 1998.

Stevenson, R.E., A view from space: the discovery of nonlinear waves in the ocean's near surface layer. *21st Century Sci. Technol., 12*, 34-47, 1999.

Stuart, J.T., On finite amplitude oscillations in laminar mixing layers. *J. Fluid Mech., 29*, 417-440, 1967.

Tennekes, H., and J.L. Lumley, *A First Course in Turbulence.* MIT Press, 1972.

This preprint was prepared with AGU's LaTeX macros v4, with the extension package 'AGU^{++}' by P. W. Daly, version 1.6a from 1999/05/21, with modifications by D. E. Kelley, version 1.0 from 2001/03/26, for the *'Aha Huliko'a* Hawaiian Winter Workshop.